Planarity and Constraint of the Carbonyl Groups in 1,2-Diones Are Determinants for Selective Inhibition of Human Carboxylesterase 1

Janice L. Hyatt,[†] Randy M. Wadkins,[‡] Lyudmila Tsurkan,[†] Latorya D. Hicks,[†] M. Jason Hatfield,[†] Carol C. Edwards,[†] Charles R. Ross II,[§] Stephanie A. Cantalupo,[||] Guy Crundwell,[||] Mary K. Danks,[†] R. Kip Guy,[⊥] and Philip M. Potter*[,†]

Department of Molecular Pharmacology, St. Jude Children's Research Hospital, Memphis, Tennessee 38105, Department of Chemistry and Biochemistry, University of Mississippi, University, Mississippi 38677, Department of Structural Biology, St. Jude Children's Research Hospital, Memphis, Tennessee 38105, Department of Chemistry and Biochemistry, Central Connecticut State University, New Britain, Connecticut 06050, and Department of Chemical Biology and Therapeutics, St. Jude Children's Research Hospital, Memphis, Tennessee 38105

Received June 12, 2007

Carboxylesterases (CE) are ubiquitous enzymes responsible for the detoxification of xenobiotics, including numerous clinically used drugs. Therefore, the selective inhibition of these proteins may prove useful in modulating drug half-life and bioavailability. Recently, we identified 1,2-diones as potent inhibitors of CEs, although little selectivity was observed in the inhibition of either human liver CE (hCE1) or human intestinal CE (hiCE). In this paper, we have further examined the inhibitory properties of ethane-1,2-diones toward these proteins and determined that, when the carbonyl oxygen atoms are *cis*-coplanar, the compounds demonstrate specificity for hCE1. Conversely, when the dione oxygen atoms are not planar (or are *trans*-coplanar), the compounds are more potent at hiCE inhibition. These properties have been validated in over 40 1,2-diones that demonstrate inhibitory activity toward at least one of these enzymes. Statistical analysis of the results confirms the correlation ($P < 0.001$) between the dione dihedral angle and the preferential inhibition of either hiCE or hCE1. Overall, the results presented here define the parameters necessary for small molecule inhibition of human CEs.

Introduction

Carboxylesterases (CEs[a]) are ubiquitous enzymes responsible for the detoxification of xenobiotics.[1] They cleave carboxylesters (RCOOR′) into the corresponding carboxylic acid (RCOOH) and alcohol (R′OH). Because numerous clinically used drugs contain the ester chemotype, a moiety known to improve water solubility and allow development of prodrug formulations, the expression of these proteins can modulate the bioavailability of these agents. Additionally, CEs demonstrate promiscuous catalytic activity and can also hydrolyze carbamates, thioesters, and amides. As a result, numerous drugs are substrates for these enzymes. These include meperidine (Demerol), cocaine, heroin, β-flestolol, CPT-11 (irinotecan), capecitabine, procaine (Novocaine), and lidocaine.[2−9] Consequently, the levels and tissue distribution of CE expression will impact the disposition of these agents.

In humans, two predominant CEs are expressed. hCE1 is primarily present in the liver and is efficacious in the hydrolysis of relatively small molecules (e.g., *o*-nitrophenyl acetate (*o*-NPA)).[10] In contrast, hiCE (hCE2), which is expressed in the intestine and the liver, can hydrolyze large bulky substrates, such as the anticancer agent CPT-11.[11,12] Because hiCE is overexpressed in the intestine and the dose limiting toxicity for CPT-11 is diarrhea, potentially, inhibition of this protein may ameliorate the toxicity associated with drug treatment. Therefore, we have recently undertaken a series of studies designed to identify and characterize selective CE inhibitors.[13−18] These experiments indicated that ethane-1,2-dione-containing compounds could selectively inhibit CEs and demonstrated no inhibition of human acetyl- or butyrylcholinesterase (hAChE and hBChE, respectively).[14,15,17] The benzil-based compounds were very potent CE inhibitors, with inhibition constant (K_i) values for enzyme inhibition in the low nM range. In addition, while the mode of enzyme inhibition for these compounds was partially competitive, hydrolysis of a variety of different substrates was reduced, suggesting that these benzil analogues may have utility in modulating turnover of many different ester-containing drugs. Interestingly, out of over 30 ethane-1,2-dione-containing compounds that were analyzed, all demonstrated more potent inhibition of hiCE as compared to hCE1.[17]

During the course of these studies, it became apparent that compounds containing the 1,2-dione moiety, where the carbonyl carbon atoms were fused within a ring structure, were also potent CE inhibitors. However, these compounds demonstrated specificity for hCE1 as compared to hiCE. In this manuscript, we have further characterized these inhibitors and determined that, when the oxygen atoms in the 1,2-dione moiety are *cis*-coplanar, the molecule demonstrates preferential inhibition of hCE1. In contrast, when the dihedral angle between the oxygen atoms is greater than 10°, the compounds are more potent at inhibiting hiCE. This has led to the design and synthesis of thieno[3,2-*e*][1]benzothiophene-4,5-dione, which demonstrates preferential inhibition of hCE1 (K_i = 150 nM) as compared to hiCE (K_i = 850 nM), but is inactive toward hAChE or hBChE.

* To whom correspondence should be addressed. Dr. Philip M. Potter, Department of Molecular Pharmacology, St. Jude Children's Research Hospital, 332 N. Lauderdale, Memphis, TN 38105-2794. Tel.: 901-495-3440. Fax: 901-521-1668. E-mail: phil.potter@stjude.org.

[†] Department of Molecular Pharmacology, St. Jude Children's Research Hospital.

[‡] Department of Chemistry and Biochemistry, University of Mississippi.

[§] Department of Structural Biology, St. Jude Children's Research Hospital.

[||] Department of Chemistry and Biochemistry, Central Connecticut State University.

[⊥] Department of Chemical Biology and Therapeutics, St. Jude Children's Research Hospital.

[a] Abbreviations: CE, carboxylesterase; CSD, Cambridge Structural Database; CPT-11, irinotecan; DMSO, dimethyl sulfoxide; hAChE, human acetylcholinesterase; hBChE, human butyrylcholinesterase; hCE1, human carboxylesterase 1; hiCE, human intestinal carboxylesterase; K_i, inhibition constant; Mp, melting point; *o*-NPA, *o*-nitrophenyl acetate.

10.1021/jm0706867 CCC: $37.00
Published on Web 10/17/2007

Materials and Methods

Chemicals. Solvent and reagents for general synthesis were purchased from Sigma-Aldrich (St. Louis, MO) or TCI America (Portland, OR). Sources for the commercially available compounds used for enzyme inhibition analyses are indicated in Table 1.

Enzymes. Pure hCE1 and hiCE were prepared from serum-free *Spodoptera frugiperda* Sf9 media, as previously described.[19] hAChE and hBChE were purchased from Sigma Biochemicals (St. Louis, MO).

Chemistry. Melting points (Mps) were determined using a Meltemp (Barnstead International, Dubuque, IA), IR spectra were obtained using thin films dried on KBr discs using an IR100 FT-IR spectrometer (Thermo Electron Co., Waltham, MA), and UV spectra were determined in dichloromethane or DMSO using a DU 640 (Beckmann Coulter, Fullerton, CA). The purity and structure of synthesized compounds were determined by TLC, NMR, MS, and total C, H, N, O, and S analysis. X-ray structure coordinates for selected molecules were obtained from the Cambridge Structural Database (CSD) and were visualized using ICM-Pro software (Molsoft L.L.C., La Jolla, CA).

Synthesis of 1,2-Dicyclohexylethane-1,2-dione (7). 1,2-Dicyclohexylethane-1,2-dione (**7**) was synthesized as previously described by the reaction of cyclohexyl magnesium bromide with oxalyl chloride.[20] Physical and structural parameters were consistent with those previously reported (physical parameters for compound **7** are provided as Supporting Information).

Synthesis of Thieno[3,2-*e*][1]benzothiophene-4,5-dione (19). Thieno[3,2-*e*][1]benzothiophene-4,5-dione (**19**) was synthesized from 3,3-bithiophene and oxalyl chloride as detailed by Phillips et al.[21] Physical and structural parameters were consistent with those previously reported (physical parameters for compound **19** are provided as Supporting Information).

LogP Calculation. LogP values were calculated using ChemSilico Predict v2.0 software (ChemSilico LLC, Tewksbury, MA).

Carboxylesterase Inhibition. CE activity assays and enzyme inhibition were determined using 3 mM *o*-NPA as a substrate, as reported previously.[17,18,22]

Acetylcholinesterase and Butyrylcholinesterase Inhibition. The inhibition of hAChE and hBChE was assessed as previously reported by Wadkins et al.[17,18]

Determination of K_i Values. K_i values for enzyme inhibition were performed as described previously.[17,18] Briefly, inhibition data were fitted to the following equation[23]

$$i = \frac{[I]\{[s](1-\beta) + K_s(\alpha-\beta)\}}{[I]\{[s] + \alpha K_s\} + K_i\{\alpha[s] + \alpha K_s\}}$$

where i = fractional inhibition, $[I]$ = inhibitor concentration, $[s]$ = substrate concentration, α = change in affinity of substrate for enzyme, β = change in the rate of enzyme substrate complex decomposition, K_s is the dissociation constant for the enzyme substrate complex, and K_i is the inhibitor constant. Examination of the curve fits, where α ranged from 0 to ∞ and β ranged from 0 to 1, was performed using Perl Data Language and GraphPad Prism software. The curves generating the highest r^2 value for the fits were analyzed using Akaike's information criteria,[24,25] and subsequent statistical analysis was then performed to assign the mode of enzyme inhibition. K_i values were then calculated from these data sets.

Determination of 1,2-Dione Dihedral Angle. For compounds that had been previously crystallized and subjected to X-ray diffraction analysis (**1**−**6**, **10**, **14**, **17**, **18**), the [(O)CC(O)] dione dihedral angle was taken directly from coordinates of the structures. For other compounds, the angle was predicted using computer-assisted geometry optimization of the structures. Briefly, compounds were constructed in Gauss-View and geometry optimizations were performed at the B3LYP/6-31G(p,d) level of theory.[26,27] These procedures were performed with Gaussian 03 software[28] (Gaussian, Wallingford, CT) on a dual Xeon 3.2GHz computer running Microsoft Windows XP.

Table 1. Structures, Names, and Sources of the Compounds Assayed in This Paper

ID	Structure	Name	Source
1	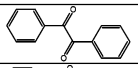	Benzil (diphenylethane-1,2-dione)	Sigma Aldrich
2	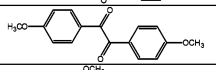	4,4'-Dimethoxybenzil (1,2-bis(4-methoxyphenyl)ethane-1,2-dione)	Sigma Aldrich
3	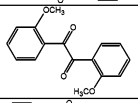	2,2'-Dimethoxybenzil (1,2-bis(2-methoxyphenyl)ethane-1,2-dione)	ChemDiv (San Diego, CA)
4	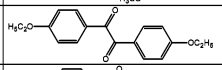	4,4'-Diethoxybenzil (1,2-bis(4-ethoxyphenyl)ethane-1,2-dione)	ChemDiv
5	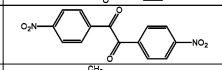	4,4'-Dinitrobenzil (1,2-bis(4-nitrophenyl)ethane-1,2-dione)	ChemDiv
6	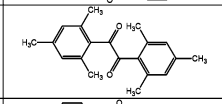	Mesitil (1,2-bis-(2,4,6-trimethylphenyl)-ethane-1,2-dione)	Aurora (Graz, Austria)
7	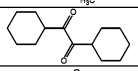	1,2-Dicyclohexylethane-1,2-dione	This paper [20]
8	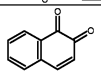	1,2-Naphthoquinone	Sigma Aldrich
9	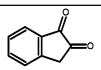	1,2-Indanedione	Tyger (Ewing, NJ)
10		Acenaphthoquinone	Sigma Aldrich
11	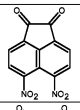	5,6-Dinitroacenaphthoquinone	Sigma Aldrich
12		5,6-dihydro-4*H*-pyrrolo[3,2,1-*ij*] quinoline-1,2-dione	Aurora
13	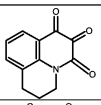	6,7-Dihydro-1*H*,5*H*-pyrido[3,2,1-*ij*] quinoline-1,2,3-trione	Aurora
14	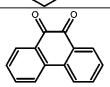	Phenanthrene-9,10-dione	Sigma Aldrich
15	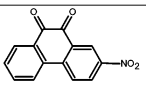	2-Nitro-phenanthrene-9,10-dione	Sigma Aldrich
16	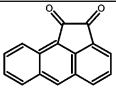	Aceanthrene-9,10-dione	Sigma Aldrich
17	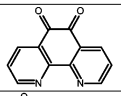	1,10-Phenanthroline-5,6-dione	Sigma Aldrich
18	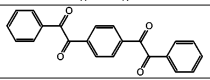	Bisbenzil (2,2'-diphenyl-1,1'-(1,4-phenylene)diethanedione)	TCI America
19	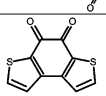	Thieno[3,2-e][1] benzothiophene-4,5-dione	This paper [21]
20	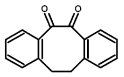	11,12-Dihydro-dibenzo[a,e]cyclooctene-5,6,dione	MDPI (Basel, Switzerland)
21	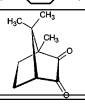	(±)-camphorquinone ((4*S*)-1,7,7-trimethylbicyclo[2.2.1] heptane-2,3-dione)	Sigma Aldrich

Crystal Structure Determination. The crystal structure of **19** was determined from single-crystal X-ray diffraction omega scan data collected at 298 K on an Oxford Diffraction Xcalibur equipped

Table 2. Dihedral Angles of the O−C−C−O Bond, IR Wave Numbers for the C═O Bond, and K_i Values for Esterase Inhibition for the 1,2-Dione-Based Compounds

	O−C−C−O dihedral (°)					K_i values for enzyme inhibition (nM)			
ID	X-ray structure[a] (CSD file)	MO	cLogP	UV n to π^* (nm)	IR C═O (cm^{-1})	hiCE	hCE1	hAChE	hBChE
1	107.8 (BENZIL) [98][b]	132.9	3.02	382	1660	14.7 ± 1.9[c]	148 ± 28[c]	>100 000	>100 000
2	123.1 (CASGEI)	136.0	3.49	299	1656	70.2 ± 1.1[c]	3,410 ± 550[c]	>100 000	>100 000
3	103.5 (JAVLEX)	95.2	3.28	315	1656	>100 000	>100 000	>100 000	>100 000
4	97.8 (CASGIM01)	135.5	4.16	301	1655	1420 ± 390	>100 000	>100 000	>100 000
5	111.5 (DNBZIL)	138.2	2.54	278	1680	470 ± 60	9800 ± 1200	>100 000	>100 000
6	178.3 (BOLCUA)	123.8	5.42	465 492	1699	4040 ± 1020	>100 000	>100 000	>100 000
7	172[d]	179.0	3.93	438	1706	5.0 ± 0.7	72 ± 5	>100 000	>100 000
8	ND[e]	0	1.09	400	1666	2400 ± 600	930 ± 280	320 ± 16	2290 ± 450
9	ND	0	0.87	484	1710	5470 ± 530	5240 ± 860	>100 000	2630 ± 40
10	1.0 (ACNAQU)	0	2.24	482	1719	170 ± 22	31 ± 4	>100 000	2970 ± 580
11	ND	0	2.01	322	1747	620 ± 160	570 ± 96	903 ± 130	3100 ± 400
12	ND	−0.1	0.84	434	1728	4130 ± 570	1540 ± 540	>100 000	>100 000
13	ND	3.3 −2.2	0.72	324	1628	>100 000	5380 ± 660	>100 000	>100 000
14	3.13 (ZZIYEO1)	0	2.79	415	1673	52 ± 3	2.5 ± 0.2	>100 000	190 ± 50
15	ND	0.1	2.41	399	1672	107 ± 7	15.9 ± 0.7	850 ± 90	1670 ± 290
16	ND	0	3.42	402	1704	7.7 ± 0.4	1.5 ± 0.1	>100 000	>100 000
17	3.4 (MEJWED)	0	1.12	454	1686	>100 000	5400 ± 1000	>100 000	>100 000
18	−111.6 111.6 (CIJFIK)	−133.4 133.4	3.53	400	1671	5.6 ± 0.4[c]	8.0 ± 0.9[c]	>100 000	>100 000

[a] As determined from the CSD file for the respective compound. [b] The dihedral angle of benzil in solution is 98°.[41] [c] Data taken from Wadkins et al.[17] [d] Calculated based on the correlation between the wave number and the dihedral angle for a series of nonconjugated cyclic 1,2-diketones.[42,43] [e] ND: not determined.

with a Sapphire 3 CCD detector and a fine-focus sealed tube Mo Kα X-ray source (λ = 0.710 73 Å). Data were corrected for absorption effects using SADABS[29] and the observed R_{int} was 0.0322. Data workup, structure solution, refinement, and the generation of cif files were performed using SHELXTL.[30] All nonhydrogen atoms were identified from initial direct methods solutions and refined anisotropically. Hydrogen atoms were found in subsequent difference maps and were allowed to refine isotropically. All bond lengths and angles fell within normal, expected values. The final R_1 value was 0.0347. The full details of crystal structure determinations, such as data collection parameters, all bond lengths, and refinement statistics, are available as Supporting Information.

Statistical Analysis. Data were analyzed using GraphPad Prism software. Three independent analyses were performed; linear regression, Spearman rank order correlations, and Fisher's exact tests from contingency tables. In the latter, samples were grouped based upon a dihedral angle of <10° or >10° and were tabulated against which enzyme (hiCE or hCE1) was preferentially inhibited. In all analyses, $P < 0.05$ was considered statistically significant.

3D-QSAR Modeling of Carboxylesterase Inhibitors. The generation of 3D-QSAR models for the inhibition of the CEs by the compounds described here were performed as previously described.[16−18,31] Structures for each analogue were taken from the minimized structures from Gaussian 03 that were used to derive the [(O)CC(O)] dihedral angles. To be consistent with earlier QSAR studies, Gaussian 03 partial charges were not used. Instead, partial atomic charges from the bond charge correction method[32] and AMBER atom types were assigned using the *antechamber* module of AMBER9 (University of California, San Francisco, CA). All analogues were aligned using the [(O)CC(O)] dihedral of benzil as a template and analyses were then performed using Quasar 5.0 software.[33−36] This program produced a receptor surface model based upon 200 independent structures for each data set. These were then cross-validated to yield ~7000 pseudoreceptor site models that, upon further analysis, routinely yielded cross-correlation coefficients (q^2) that exceeded 0.9 for the predicted versus the observed K_i values. This usually resulted in linear correlation coefficients (r^2) of >0.8.

Results and Discussion

Inhibition of CEs by 1,2-Dione Containing Compounds. We have previously evaluated the ability of over 30 benzil analogues to inhibit human CEs.[17] All of these compounds demonstrated preferential inhibition of hiCE as compared to hCE1, with K_i values as low as 4 nM being observed. These studies indicated that substitution within the benzene rings altered inhibitor potency; however, these substitutions did not change the preferential inhibition of hiCE.[17] To further our analysis of ethane-1,2-dione-mediated inhibition of mammalian CEs, we obtained and synthesized a series of compounds in which the carbonyl groups were either free to rotate or constrained. These molecules were chosen based on their availability and their physical characteristics (aromatic, nonaromatic, planar, nonplanar, etc) as we have previously reported that these properties are important determinants for CE inhibition.[14] The structures of these molecules are shown in Table 1.

The K_i values for hiCE and hCE1 inhibition are shown in Table 2. As can be seen, compounds in which the carbonyl groups are *cis*-coplanar (**8**−**17**), are more potent inhibitors of hCE1 as compared to hiCE. In contrast, molecules in which the carbonyl moieties are *trans*-coplanar (i.e., **7**) or are nonplanar

Table 3. Statistical Correlations between Physical Parameters of the Dione Inhibitors and Enzyme Inhibition. Statistically Significant Values Are Indicated in Bold.

		parameter					
statistical analysis	enzyme	cLogP vs K_i	IR C═O wave number vs K_i	O−C−C−O dihedral (X-ray) vs K_i[a]	O−C−C−O dihedral (MO) vs K_i	O−C−C−O dihedral <10° vs K_i	O−C−C−O dihedral >10° vs K_i
linear regression (r^2)	hiCE	0.206	0.166	0.084	0.035	NA[b]	NA
	hCE1	0.000	0.067	0.152	0.143	NA	NA
Spearman correlation (P value)	hiCE	**0.021**	0.704	0.435	0.134	NA	NA
	hCE1	0.951	0.173	0.485	0.296	NA	NA
contingency table (P value)	hiCE	NA	NA	NA	NA	NA	**0.0002**
	hCE1	NA	NA	NA	NA	**0.0002**	NA

[a] Analysis was only performed with compounds with known dihedral angles. [b] Not applicable.

(**1**−**6** and **18**) demonstrate preferential inhibition of hiCE. Interestingly, compound **3** (nonplanar) was not an inhibitor of either CE, whereas **4** (nonplanar) was selective for hiCE and **17** (*cis*-coplanar) only inhibited hCE1.

Analysis of the [(O)CC(O)] Bond Dihedral Angle in Selected 1,2-Diones. The dihedral angle of the [(O)CC(O)] bond in the majority of the compounds was determined via two different approaches. First, the CSD was searched with the target molecules and the dihedral angle was calculated from the deposited coordinates. Routinely, angles were determined from datasets performed at room temperature. The dihedral angles obtained from the CSD files are indicated in Table 2.

As a corollary to these studies, we also determined the dihedral angle using molecular orbital calculations. These analyses were performed using the B3LYP/631G formalism. The calculated values of the dihedral angle of the [(O)CC(O)] bond were accurately predicted for the cyclohexyl derivative (**7**) and the polycyclic aromatic compounds (**8**, **10**, **14**, and **17**). However, for the benzil analogues (**1**−**6**, **18**), the calculated angle of this bond was ∼30° greater than the actual values obtained from the crystallographic studies. The reason for this discrepancy is unclear, but because the error was similar in all cases (i.e., always ∼30° greater than the actual value), this may represent an anomaly in the Gaussian energy minimization routines. We have analyzed the crystal structures of the benzil analogues and determined that there is a tendency for the torsion angle to be decreased such that the aromatic rings can be stacked in the crystal. This would be a favorable interaction resulting in a lower energy state. However, interaction with other molecules in the crystal also occurs (e.g., the carbonyl carbon in 4,4′-dimethoxybenzil is in close proximity to the methyl group of another molecule). In general, these interactions tend to reduce the dihedral angle of the [(O)CC(O)] bond, which would not be apparent from the MO calculations.

Since we have demonstrated that the CE-inhibitory properties of isatins can, in part, be predicted by the logP of the molecule, we calculated this parameter and assessed whether these values correlated with the K_i values for the proteins. Interestingly, using Spearman rank analysis, we observed a correlation between the clogP and the K_i values for hiCE ($P = 0.021$; Table 3), but not with hCE1 ($P = 0.951$). Hence, it would appear for the former enzyme that the hydrophobicity of the inhibitor contributes significantly to interaction with these molecules. Conversely, this appears not to be the case for hCE1.

We also determined the IR frequency for the absorption by the C═O bond in the 1,2-diones. These analyses were performed because it is known that the wavelength of this signal is dependent upon several factors, including ring strain, hydrogen bonding, and conjugation. However, attempts to correlate the wave number for this vibration with the observed K_i values for enzyme inhibition were unsuccessful (Tables 2 and 3).

Finally, we determined the *n*-to-π^* transition for these 1,2-diones by UV spectroscopy. Because a bathochromic shift occurs as the dihedral angle between the carbonyl groups approaches 90°, this method of analysis can be used to assess the planarity of the diones. Consistent with this hypothesis, we observed a correlation between the predicted dihedral angle from the MO calculations and the *n*-to-π^* transition for the unconjugated diones (**1** − **7**, **18**), yielding an r^2 value of 0.74 (data not shown). However, no such correlation was observed with compounds **8**−**17** or **19**−**21**. Consequently, we did not perform statistical analyses comparing the UV absorption values with the K_i constants for the different enzymes.

Benzil and its analogues usually adopt a nonplanar conformation due to steric constraints. This is primarily due to steric clashes between the oxygen atoms and the hydrogens in the *ortho*-position of the benzene rings. In contrast, in the dicyclohexane derivative (**7**), the [(O)CC(O)] dihedral angle is nearly 180° (i.e., *trans*-coplanar; Table 2), presumably because the oxygen atoms do not clash with the ring hydrogens due to the chair conformations that are adopted by the cyclohexane rings. However, despite this difference, both benzil (**1**) and 1,2-dicyclohexylethane-1,2-dione (**7**) are potent inhibitors of the human CEs and demonstrate selectivity for hiCE. In contrast, the molecules that contain the 1,2-dione moiety held in a rigid, coplanar *cis*-configuration by the aromatic ring systems (compounds **8**−**17** and **19**), are more potent inhibitors of hCE1.

Correlation between the K_i Values for CE Inhibition and the 1,2-Dione Dihedral Angle. As indicated in Table 2, compounds that had a [(O)CC(O)] dihedral angle of less than 10° (i.e., the O atoms were *cis*-coplanar) were more potent inhibitors of hCE1 than hiCE. This is exemplified by all of the compounds that contain the dione moiety constrained within the planar aromatic rings (inhibitors **8**−**17**). Conversely, all compounds that contained the carbonyl groups at a dihedral angle greater than 10° were more potent inhibitors of hiCE. This includes the 1,2-diones assayed in this paper (**1**, **2**, **4**−**7**, and **18**) as well as all of the benzil analogues that we have previously analyzed.[17]

Statistical analysis of these results using contingency tables comparing K_i values for either hiCE or hCE1 inhibition, with a dihedral angle of less than or greater than 10°, resulted in significant correlations with $P = 0.0002$ (Table 3). However, no correlations were observed with the actual angle versus the K_i values either using linear regression or by Spearman rank order analyses (Table 3). Additionally, statistically significant correlations using the contingency table analysis were also observed with the 43 additional benzil-based inhibitors that have

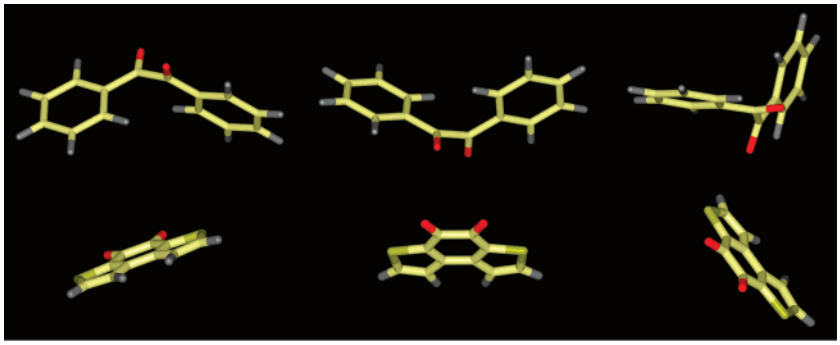

Figure 1. Oblique views of the structures of benzil (**1**; upper panel) and thieno[3,2-*e*][1]benzothiophene-4,5-dione (**19**; lower panel). The dihedral angle between the oxygen atoms (red) is 107.8° for **1** and 0.4° for **19**. Models were generated from the coordinates obtained from X-ray crystallographic analyses of the molecules.

Table 4. Physical Parameters and K_i Values for Esterase Inhibition for 11,12-Thieno[3,2-*e*][1]benzothiophene-4,5-dione (**19**), 11,12-Dihydrodibenzo[*a*,*e*]cyclooctene-5,6,dione (**20**) and (±)-Camphorquinone (**21**)

	O−C−C−O dihedral (°)					K_i values for enzyme inhibition (nM)			
ID	X-ray structure	MO	cLogP	UV *n* to π^* (nm)	IR C=O (cm^{-1})	hiCE	hCE1	hAChE	hBChE
19	0.4	0	2.65	467	1650	850 ± 150	150 ± 30	>100 000	>100 000
20	ND	56	2.75	259	1671	6150 ± 2080	2980 ± 280	>100 000	>100 000
21	14[a]	0.4	1.77	468	1750	>100 000	>100 000	>100 000	>100 000

[a] Calculated based upon the dipole moment.[43]

previously been demonstrated to be CE-specific inhibitors (data not shown).[13,17]

Molecular modeling studies using these analogues with the X-ray coordinates for hCE1, demonstrated no dramatic differences in the ability of either the planar or nonplanar inhibitors to interact with the catalytic amino acids in the protein (data not shown). In general, after docking the compounds with the lower K_i values, positioned such that the carbonyl carbon atoms were closer to the serine Oγ, there was no statistical significance between these distances and the K_i values (data not shown). We have been unable to perform similar studies with hiCE as the structure of this protein has not been solved. However, these modeling experiments suggest that it is not the direct interaction of the serine nucleophile with the carbonyl carbon atom that is important for CE inhibition, but rather other factors dependent upon the protein structure. For example, the catalytic triad of amino acids in the mammalian CEs (Ser, His, and Glu) are buried at the bottom of a long narrow gorge that projects ~20 Å into the protein.[10,37−39] Enzyme inhibition, therefore, will be dependent upon the ability of the small molecule to diffuse into the gorge and access the catalytic residues. Hence, larger, more bulky, molecules would likely be poorer CE inhibitors. In addition, it is known that the plasticity of the loops of amino acids that form the entrances to the active site gorge modulate substrate hydrolysis.[10] Consequently, inhibitors that demonstrate less flexibility may demonstrate preferential inhibition of one enzyme versus another.

Attempts To Design an hCE1-Specific Inhibitor. Our previous studies indicated that substitution of the benzene rings in benzil with heteroaromatic moieties (e.g., thiophene or pyridine) resulted in compounds that demonstrated similar K_i values for the inhibition of hiCE and hCE1.[14] In addition, substitution of nitrogen within the fused aromatic rings of phenanthrene-9,10-dione (**14**) to yield 1,10-phenanthroline-5,6-dione (**17**) resulted in the dramatic reduction of the inhibitory potency toward hiCE (Table 2). Therefore, we postulated that a *cis*-coplanar dicarbonyl compound, which contained heteroatoms, such as sulfur, as part of a fused aromatic system might be an effective, selective inhibitor of hCE1. In addition, we hypothesized that this compound would be a poor inhibitor of hiCE. Consequently, we synthesized such a compound (thieno-[3,2-*e*][1]benzothiophene-4,5-dione; **19**) by the simple condensation of 3,3′-bithiophene with oxalyl chloride.[21] MO calculations of **19** indicated that the [(O)CC(O)] dihedral angle was 0°, and this was confirmed by X-ray crystallographic studies (0.4°; Table 4; Figure 1). Biochemical assays with compound **19** indicated that this molecule demonstrated preferential inhibition for hCE1 (K_i = 150 nM) as compared to hiCE (K_i = 850nM) or the human cholinesterases (Table 4). While not exclusively selective for hCE1, these results confirmed our hypothesis that planar compounds containing heteroatoms may be used as scaffolds for the development of CE inhibitors.

Because selectivity for hCE1 was observed with the *cis*-coplanar molecules, we envisage, therefore, that the hCE1 active site gorge and its associated entrance adopts an oval conformation (in cross section), that allows the access of relatively narrow molecules to the catalytic amino acids. In hiCE, it is likely that the gorge is more rounded and can readily accommodate wider molecules. For example, in its most stable conformation, benzil (**1**) maintains a diameter of ~4.6 Å (Figures 1 and 2). This compound inhibits both CEs, but is 10 times more potent toward hiCE than hCE1. In contrast, thieno [3,2-*e*][1]benzothiophene-4,5-dione (**19**) is ~1.0 Å (1.85 Å Van der Waals radius) at its widest part (the diameter of the sulfur atom; Figures 1 and 2) and is an excellent inhibitor of hCE1, but demonstrates weaker activity against hiCE. Hence, it is likely that the discrimination of molecules that can enter the active site gorge of hCE1 is primarily mediated by their overall diameter and shape. As a consequence, narrow, *cis*-coplanar 1,2-dione-containing molecules are better inhibitors of this protein as compared to hiCE. Clearly, however, benzil (**1**) can change its conformation and access the catalytic amino acids in hCE1, because we have observed enzyme inhibition by this compound. However, due to the constraints enforced by the thiophene rings in **19**, we would predict that this compound cannot adopt an alternate conformation, and this rigidity dictates specificity for hCE1.

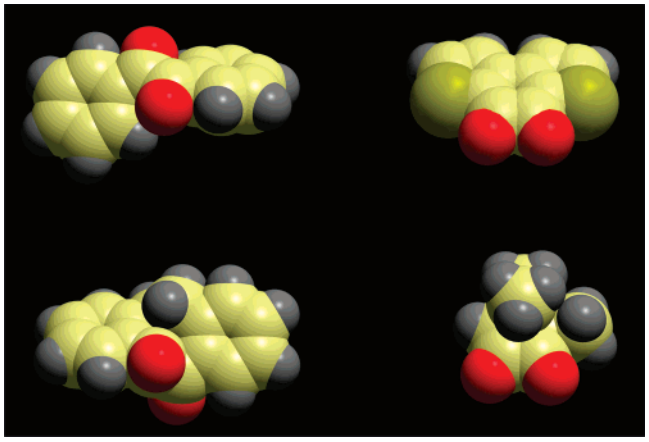

Figure 2. CPK images of some of the compounds discussed in this paper: upper left, benzil (**1**); upper right, thieno[3,2-*e*][1]benzothiophene-4,5-dione (**19**); lower left, dibenzo[*a*,*e*]cyclooctene-5,6,dione (**20**); lower right, (+)-camphorquinone (**21**).

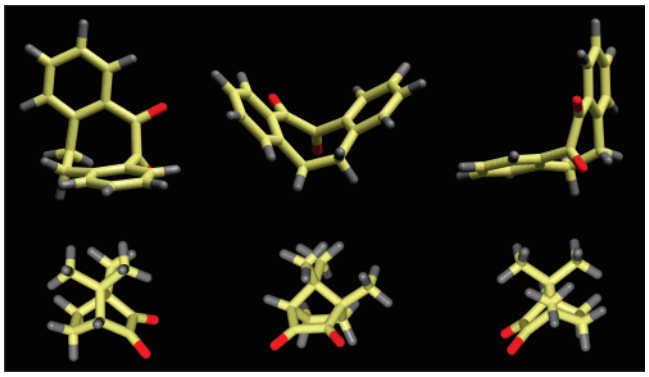

Figure 3. Oblique views of the structures of 11,12-dihydrodibenzo-[a,e]cyclooctene-5,6,dione (**20**; upper panel) and (+)-camphorquinone (**21**; lower panel). For **20**, the dihedral angle between the oxygen atoms (red) is 56.0° and the planar angle between the benzene rings is 104.7°. For **21**, the dihedral angle is 0.4°. Models were generated from the lowest energy conformations, as determined by MO calculations.

Is Effective hCE1 Inhibition in the *cis*-Coplanar Compounds Mediated by the Dione Moiety or the Aromaticity of the Molecules? We have previously reported that the inhibition of CEs by substituted ethane-1,2-diones is in part mediated by the aromaticity of the substituents.[14] Therefore, the increased potency of the planar inhibitors toward hCE1 may be due to the aromatic nature of these compounds rather than the dihedral angle of the dione moiety. In an attempt to address this issue, we determined the ability of 11,12-dihydrodibenzo-[*a*,*e*]cyclooctene-5,6,dione (**20**) to inhibit the human CEs. This compound adopts a pseudo-boat conformation with a computer-predicted [(O)CC(O)] dihedral angle of 56° (Figure 3). The central octane ring is flanked by two benzene rings, thereby maintaining the aromatic nature of the compound molecule; however, because the latter are at angles of 104.7° to each other, the molecule lacks planarity. Hence, by comparison of the K_i values for CE inhibition for this compound with phenanthrene-9,10-dione (**14**), it should be possible to determine whether planarity or aromaticity predominates toward hCE1 inhibition. As indicated in Table 4, **20** was a poor inhibitor of hiCE but demonstrated greater potency toward hCE1. Indeed, this compound was ~2-fold better at inhibiting hCE1 as compared to hiCE, although the actual K_i values were relatively high (2.98 ± 0.28 μM and 6.15 ± 2.08 μM for hCE1 and hiCE, respectively). We also assayed (±)-camphorquinone (**21**) because this 1,2-dione is nonplanar and also lacks an aromatic component (Figure 3). However, this molecule was completely ineffective as an inhibitor of either the human CEs or the cholinesterases (Table 4).

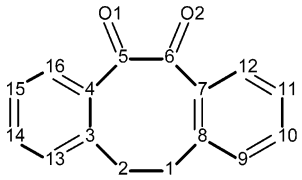

Figure 4. Numbering scheme for atoms in 11,12-dihydrodibenzo[a,e]-cyclooctene-5,6,dione (**20**).

It is likely that compound **20** (11,12-dihydrodibenzo[*a*,*e*]-cyclooctene-5,6-dione) is a less-potent inhibitor than the other 1,2-diones because the molecule is constrained into a boat conformation (Figure 3). Because the catalytic amino acids of CEs are buried at the bottom of a long-active site gorge, for enzyme inhibition to occur, the small molecule must be able to readily access these residues. The somewhat rigid conformation adopted by **20** would impede the ability of the inhibitor to reach the active site serine, thereby mitigating the efficacy of inhibition. In addition, attack of the carbonyl carbon atoms (C5 and C6; Figure 4) by the serine nucleophile is likely to be hindered due to the configuration of **20** that forces the target carbon atoms upward. Attack by the O^- would have to occur between the benzene rings because access to the carbonyl carbon atoms would be shielded by the oxygen atoms (O1 and O2) and the methylene carbons (C1 and C2) and their associated hydrogen atoms, which form part of the octane ring. Such impedance would not occur with the *cis*-coplanar inhibitor molecules (e.g., **14** and **19**), allowing them to more efficiently inhibit the CEs.

Camphorquinone (**21**) exists as either the (+)- or (−)-enantiomers (dependent upon the position of the methyl group attached to the cyclohexane ring) and both adopt a pseudo-boat (or inverted "V") formation (Figure 3). However, dipole moment and MO calculations indicate that the [(O)CC(O)] dihedral angle is 14 or 0.4°, respectively, and this cannot change due to the constraint provided by the methylene carbon atoms. Hence, free rotation around the bond connecting the carbonyl carbon atoms is eliminated. As the oxygen atoms are *cis*-coplanar, this compound might be expected to be an hCE1-specific inhibitor. However, (±)-camphorquinone is inactive toward CEs (Table 4). This is likely due to the fact that the molecule is relatively bulky (Figures 2 and 3) and has a low clogP value (1.77; Table 4). It is known that the active site gorges of the mammalian CEs are highly hydrophobic due to the presence of numerous aromatic residues (Trp, Tyr, Phe).[40] Hence, molecules with higher logP values tend to be better enzyme inhibitors.[16] By comparison, the clogP values for benzil (**1**) and **19** are 3.02 and 2.65 (Tables 2 and 4), respectively. In addition, it is likely that attack of the carbonyl carbon atoms in camphorquinone by the serine nucleophile will be hindered similar to that seen with compound **20** because the target carbon atoms face the inside of the "V" structure (Figures 2 and 3). As a result, the combination of these factors yields a compound that is unable to inhibit the CEs.

3D-QSAR Pseudoreceptor Models of 1,2-Dione-Mediated Inhibition of CEs. Using the inhibition data for the series of compounds, we developed QSAR models using compounds **1**−**18** as the training set for each enzyme. Compounds **19**−**21** were then used to validate these pseudoreceptor site models. For both hiCE and hCE1, we were able to generate excellent cross correlation coefficients ($q^2 = 0.900$) for each enzyme. In addition, the linear correlations of the observed versus the

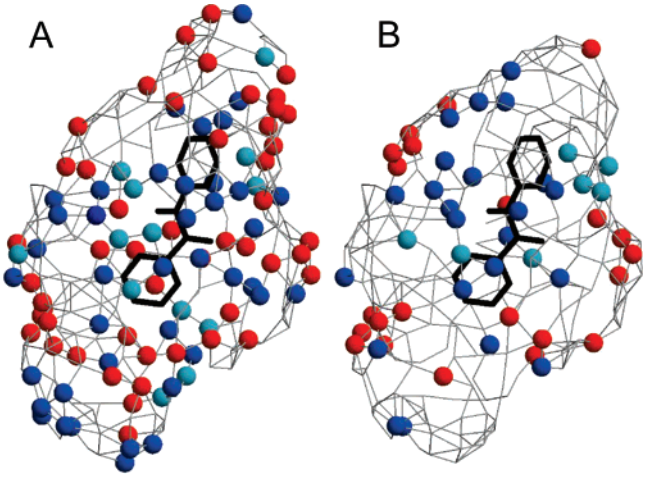

Figure 5. 3D-QSAR pseudoreceptor site models that describe the best fits for the inhibition data derived for hiCE (panel A) and hCE1 (panel B) using the 1,2-diones. In these models, the hydrophobic domains are indicated in gray, with light blue spheres representing hydrogen bond donors and dark blue spheres corresponding to regions of positive charge (+0.1e). Negatively charged (−0.1e) areas are displayed as orange-red spheres. Benzil (**1**; black) has been positioned within the model. While there is no way to ascribe a direction to these pseudoreceptor models, based on our previous studies,[13,16−18,31] we have drawn the model with the top likely oriented toward the enzyme surface and the bottom toward the catalytic active site triad. The figure was constructed and drawn using Raster3D[44] and Molscript.[45]

predicted K_i values (r^2) were 0.912 and 0.911 for hiCE and hCE1, respectively. These results indicate that these pseudoreceptor site models are likely to represent very accurate descriptors of the domains within the CE active sites that are responsible for enzyme substrate interaction.

As indicated in the QSAR models depicted in Figure 5, the charge distribution is markedly different for the two different enzymes. For example, in hiCE, it appears as though interactions occur throughout the length of the active site that influence inhibitor potency. This is exemplified by the numerous charged regions represented by the colored spheres. In contrast, with hCE1, the central core of the model is predominantly uncharged and hydrophobic (as indicated by the gray grid devoid of spheres), suggesting that this might form a suitable domain for interaction with the aromatic planar inhibitors (compounds **8**−**17**). However, it was apparent from these analyses that several compounds that were not inhibitors (i.e., had experimental K_i values >100 000 nM) were predicted to be reasonable inhibitors of the enzymes. For example, compounds **2** and **4** were predicted to be of similar inhibitory potency for both hiCE and hCE1. Experimentally, compound **4** fails to inhibit hCE1 (Table 2). We interpret this as likely due to the interaction of **4** with the active site opening or other regions of the protein that prevent it from accessing the active site. One of the pitfalls in the use of QSAR on the hydrophobic molecules used in this study is the assumption that all molecules interact with the active site in the same way and that the differences in the K_i values are due to chemical interactions within the active site. However, the pseudoreceptor models do illustrate a trend in the way the inhibitors interact with the enzymes. The benzil-like analogues (**1**−**7**) are all better inhibitors of hiCE as compared to hCE1, and the pseudoreceptor models suggest this is due to interactions distributed throughout the active site. In contrast, the planar aromatic analogues (**8**−**17**) are better inhibitors of hCE1, and this is due to the relative hydrophobic interior of the active site (Figure 5). Interestingly, although independently generated, this is qualitatively the identical result seen with fluorobenzoin inhibitors of CE, where the hCE1 QSAR model was characterized by a more hydrophobic interior.[13] The combined results of this study and Hicks et al.[13] suggest that a major reason for the variation in inhibitor activity between hiCE and hCE1 is the presence or absence, respectively, of polar interactions between the inhibitor and the enzyme active site.

Overall, our studies have identified important molecular parameters that can be used for the design of novel CE inhibitors. For all CEs, the inhibitor must contain a 1,2-dione moiety, hydrophobic domains flanking this chemotype (e.g., phenyl or cyclohexyl groups), and a relatively small molecular volume. Specificity for hiCE can be achieved by allowing the dione to rotate freely, whereas specificity for hCE1 can be accomplished by constraining the 1,2-dione in a *cis*-coplanar configuration. These properties were the basis for development of thieno [3,2-*e*][1]benzothiophene-4,5-dione (**19**), which demonstrates both potent and preferential inhibition of hCE1. These 1,2-diones will be useful tools in understanding enzyme reaction mechanisms and may be suitable as lead compounds for the design of clinically effective CE inhibitors.

Acknowledgment. We thank Dr. Tom Katz for providing an initial sample of thieno [3,2-*e*][1]benzothiophene-4,5-dione. This work was supported in part by NIH Grants CA9468, CA108775, a Cancer Center Core Grant P30 CA21765, and the American Lebanese Syrian Associated Charities.

Supporting Information Available: The full details of crystal structure determinations such as data collection parameters, all bond lengths, and refinement statistics, and the physical parameters of compounds **7** and **19**. This material is available free of charge via the Internet at http://pubs.acs.org.

References

(1) Cashman, J.; Perroti, B.; Berkman, C.; Lin, J. Pharmacokinetics and molecular detoxification. *Environ. Health Perspect.* **1996**, *104*, 23−40.
(2) Campbell, C. J.; Chantrell, L. J.; Eastmond, R. Purification and partial characterization of rat intestinal cefuroxime axetil esterase. *Biochem. Pharmacol.* **1987**, *36*, 2317−2324.
(3) Danks, M. K.; Morton, C. L.; Krull, E. J.; Cheshire, P. J.; Richmond, L. B.; Naeve, C. W.; Pawlik, C. A.; Houghton, P. J.; Potter, P. M. Comparison of activation of CPT-11 by rabbit and human carboxylesterases for use in enzyme/prodrug therapy. *Clin. Cancer Res.* **1999**, *5*, 917−924.
(4) Potter, P. M.; Pawlik, C. A.; Morton, C. L.; Naeve, C. W.; Danks, M. K. Isolation and partial characterization of a cDNA encoding a rabbit liver carboxylesterase that activates the prodrug Irinotecan (CPT-11). *Cancer Res.* **1998**, *52*, 2646−2651.
(5) Pindel, E. V.; Kedishvili, N. Y.; Abraham, T. L.; Brzezinski, M. R.; Zhang, J.; Dean, R. A.; Bosron, W. F. Purification and cloning of a broad substrate specificity human liver carboxylesterase that catalyzes the hydrolysis of cocaine and heroin. *J. Biol. Chem.* **1997**, *272*, 14769−14775.
(6) Zhang, J.; Burnell, J. C.; Dumaual, N.; Bosron, W. F. Binding and hydrolysis of meperidine by human liver carboxylesterase hCE-1. *J. Pharmacol. Exp. Ther.* **1999**, *290*, 314−318.
(7) Ahmad, S.; Forgash, A. J. Nonoxidative enzymes in the metabolism of insecticides. *Ann. Clin. Biochem.* **1976**, *13*, 141−164.
(8) Heidari, R.; Devonshire, A. L.; Campbell, B. E.; Dorrian, S. J.; Oakeshott, J. G.; Russell, R. J. Hydrolysis of pyrethroids by carboxylesterases from *Lucilia cuprina* and *Drosophila melanogaster* with active sites modified by in vitro mutagenesis. *Insect Biochem. Mol. Biol.* **2005**, *35*, 597−609.
(9) Tabata, T.; Katoh, M.; Tokudome, S.; Nakajima, M.; Yokoi, T. Identification of the cytosolic carboxylesterase catalyzing the 5′-deoxy-5-fluorocytidine formation from capecitabine in human liver. *Drug Metab. Dispos.* **2004**, *32*, 1103−1110.
(10) Wadkins, R. M.; Morton, C. L.; Weeks, J. K.; Oliver, L.; Wierdl, M.; Danks, M. K.; Potter, P. M. Structural constraints affect the metabolism of 7-ethyl-10-[4-(1-piperidino)-1-piperidino]carbonyl-oxycamptothecin (CPT-11) by carboxylesterases. *Mol. Pharmacol.* **2001**, *60*, 355−362.

(11) Humerickhouse, R.; Lohrbach, K.; Li, L.; Bosron, W.; Dolan, M. Characterization of CPT-11 hydrolysis by human liver carboxylesterase isoforms hCE-1 and hCE-2. *Cancer Res.* **2000**, *60*, 1189−1192.
(12) Khanna, R.; Morton, C. L.; Danks, M. K.; Potter, P. M. Proficient metabolism of CPT-11 by a human intestinal carboxylesterase. *Cancer Res.* **2000**, *60*, 4725−4728.
(13) Hicks, L. D.; Hyatt, J. L.; Moak, T.; Edwards, C. C.; Tsurkan, L.; Wierdl, M.; Ferreira, A. M.; Wadkins, R. M.; Potter, P. M. Analysis of the inhibition of mammalian carboxylesterases by novel fluorobenzoins and fluorobenzils. *Bioorg. Med. Chem.* **2007**, *15*, 3801−3817.
(14) Hyatt, J. L.; Stacy, V.; Wadkins, R. M.; Yoon, K. J.; Wierdl, M.; Edwards, C. C.; Zeller, M.; Hunter, A. D.; Danks, M. K.; Crundwell, G.; Potter, P. M. Inhibition of carboxylesterases by benzil (diphenylethane-1,2-dione) and heterocyclic analogues is dependent upon the aromaticity of the ring and the flexibility of the dione moiety. *J. Med. Chem.* **2005**, *48*, 5543−5550.
(15) Hyatt, J. L.; Tsurkan, L.; Wierdl, M.; Edwards, C. C.; Danks, M. K.; Potter, P. M. Intracellular inhibition of carboxylesterases by benzil: Modulation of CPT-11 cytotoxicity. *Mol. Cancer Ther.* **2006**, *5*, 2281−2288.
(16) Hyatt, J. L.; Moak, T.; Hatfield, J. M.; Tsurkan, L.; Edwards, C. C.; Wierdl, M.; Danks, M. K.; Wadkins, R. M.; Potter, P. M. Selective inhibition of carboxylesterases by isatins, indole-2,3-diones. *J. Med. Chem.* **2007**, *50*, 1876−1885.
(17) Wadkins, R. M.; Hyatt, J. L.; Wei, X.; Yoon, K. J.; Wierdl, M.; Edwards, C. C.; Morton, C. L.; Obenauer, J. C.; Damodaran, K.; Beroza, P.; Danks, M. K.; Potter, P. M. Identification and characterization of novel benzil (diphenylethane-1,2-dione) analogues as inhibitors of mammalian carboxylesterases. *J. Med. Chem.* **2005**, *48*, 2905−2915.
(18) Wadkins, R. M.; Hyatt, J. L.; Yoon, K. J.; Morton, C. L.; Lee, R. E.; Damodaran, K.; Beroza, P.; Danks, M. K.; Potter, P. M. Identification of novel selective human intestinal carboxylesterase inhibitors for the amelioration of irinotecan-induced diarrhea: Synthesis, quantitative structure−activity relationship analysis, and biological activity. *Mol. Pharmacol.* **2004**, *65*, 1336−1343.
(19) Morton, C. L.; Potter, P. M. Comparison of *Escherichia coli*, *Saccharomyces cerevisiae*, *Pichia pastoris*, *Spodoptera frugiperda*, and COS7 cells for recombinant gene expression: Application to a rabbit liver carboxylesterase. *Mol. Biotechnol.* **2000**, *16*, 193−202.
(20) Babudri, F.; Fiandanese, V.; Marchese, G.; Punzi, A. A direct access to alpha-diones from oxalyl chloride. *Tetrahedron Lett.* **1995**, *36*, 7305−7308.
(21) Phillips, K. E.; Katz, T. J.; Jockusch, S.; Lovinger, A. J.; Turro, N. J. Synthesis and properties of an aggregating heterocyclic helicene. *J. Am. Chem. Soc.* **2001**, *123*, 11899−11907.
(22) Danks, M. K.; Morton, C. L.; Pawlik, C. A.; Potter, P. M. Overexpression of a rabbit liver carboxylesterase sensitizes human tumor cells to CPT-11. *Cancer Res.* **1998**, *58*, 20−22.
(23) Webb, J. L. *Enzyme and Metabolic Inhibitors. Volume 1. General Principles of Inhibition*; Academic Press, Inc.: New York, 1963.
(24) Akaike, H. In *Information theory and an extension of the maximum likelihood principle*, Second International Symposium on Information Theory, Budapest, 1973; Petrov, B. N.; Csaki, F., Eds. Akademiai Kiado: Budapest, 1973; pp 267−281.
(25) Akaike, H. A new look at the statistical model identification. *IEEE Trans. Autom. Control* **1974**, *AC-19*, 716−723.
(26) Petersson, G. A.; Bennett, A.; Tensfeldt, T. G.; Al-Laham, M. A.; Shirley, W. A.; Mantzaris, J. A complete basis set model chemistry. I. The total energies of closed-shell atoms and hydrides of the first-row atoms. *J. Chem. Phys.* **1988**, *89*, 2193−2218.
(27) Stephens, P. J.; Devlin, F. J.; Chabalowski, C. F.; Frisch, M. J. Ab initio calculation of vibrational absorption and circular-dichroism spectra using density-functional force-fields. *J. Phys. Chem.* **1994**, *98*, 11623−11627.
(28) Frisch, M. J.; Trucks, G. W.; Schlegel, H. B.; Scuseria, G. E.; Robb, M. A.; Cheeseman, J. R.; Montgomery, J. A., Jr.; Vreven, T.; Kudin, K. N.; Burant, J. C.; Millam, J. M.; Iyengar, S. S.; Tomasi, J.; Barone, V.; Mennucci, B.; Cossi, M.; Scalmani, G.; Rega, N.; Petersson, G. A.; Nakatsuji, H.; Hada, M.; Ehara, M.; Toyota, K.; Fukuda, R.; Hasegawa, J.; Ishida, M.; Nakajima, T.; Honda, Y.; Kitao, O.; Nakai, H.; Klene, M.; Li, X.; Knox, J. E.; Hratchian, H. P.; Cross, J. B.; Bakken, V.; Adamo, C.; Jaramillo, J.; Gomperts, R.; Stratmann, R. E.; Yazyev, O.; Austin, A. J.; Cammi, R.; Pomelli, C.; Ochterski, J. W.; Ayala, P. Y.; Morokuma, K.; Voth, G. A.; Salvador, P.; Dannenberg, J. J.; Zakrzewski, V. G.; Dapprich, S.; Daniels, A. D.; Strain, M. C.; Farkas, O.; Malick, D. K.; Rabuck, A. D.; Raghavachari, K.; Foresman, J. B.; Ortiz, J. V.; Cui, Q.; Baboul, A. G.; Clifford, S.; Cioslowski, J.; Stefanov, B. B.; Liu, G.; Liashenko, A.; Piskorz, P.; Komaromi, I.; Martin, R. L.; Fox, D. J.; Keith, T.; Al-Laham, M. A.; Peng, C. Y.; Nanayakkara, A.; Challacombe, M.; Gill, P. M. W.; Johnson, B.; Chen, W.; Wong, M. W.; Gonzalez, C.; Pople, J. A. *Gaussian 03*, revision C.02; Gaussian, Inc.: Wallingford, CT, 2004.
(29) Sheldrick, G. M. *SADABS*; University of Gottingen: Gottingen, Germany, 1996.
(30) Sheldrick, G. M. *SHELXTL-Plus*; Madison, WI, 1990.
(31) Wadkins, R. M.; Hyatt, J. L.; Edwards, C. C.; Tsurkan, L.; Redinbo, M. R.; Wheelock, C. E.; Jones, P. D.; Hammock, B. D.; Potter, P. M. Analysis of mammalian carboxylesterase inhibition by trifluoromethylketone-containing compounds. *Mol. Pharmacol.* **2007**, *71*, 713−723.
(32) Jakalian, A.; Jack, D. B.; Bayly, C. I. Fast, efficient generation of high-quality atomic charges. AM1-BCC model: II. Parameterization and validation. *J. Med. Chem.* **2002**, *23*, 1623−1641.
(33) Stewart, J. J. MOPAC: a semiempirical molecular orbital program. *J. Comput.-Aided Mol. Des.* **1990**, *4*, 1−105.
(34) Vedani, A.; Dobler, M. Multidimensional QSAR: Moving from three- to five-dimensional concepts. *Quant. Struct.-Act. Relat.* **2002**, *21*, 382−390.
(35) Vedani, A.; Dobler, M. 5D-QSAR: The key for simulating induced fit? *J. Med. Chem.* **2002**, *45*, 2139−2149.
(36) Vedani, A.; Dobler, M.; Lill, M. A. Combining protein modeling and 6D-QSAR simulating the binding of structurally diverse ligands to the estrogen receptor. *J. Med. Chem.* **2005**, *48*, 3700−3703.
(37) Bencharit, S.; Morton, C. L.; Howard-Williams, E. L.; Danks, M. K.; Potter, P. M.; Redinbo, M. R. Structural insights into CPT-11 activation by mammalian carboxylesterases. *Nat. Struct. Biol.* **2002**, *9*, 337−342.
(38) Bencharit, S.; Morton, C. L.; Hyatt, J. L.; Kuhn, P.; Danks, M. K.; Potter, P. M.; Redinbo, M. R. Crystal structure of human carboxylesterase 1 complexed with the Alzheimer's drug tacrine. From binding promiscuity to selective inhibition. *Chem. Biol.* **2003**, *10*, 341−349.
(39) Bencharit, S.; Morton, C. L.; Xue, Y.; Potter, P. M.; Redinbo, M. R. Structural basis of heroin and cocaine metabolism by a promiscuous human drug-processing enzyme. *Nat. Struct. Biol.* **2003**, *10*, 349−356.
(40) Potter, P. M.; Wadkins, R. M. Carboxylesterases−detoxifying enzymes and targets for drug therapy. *Curr. Med. Chem.* **2006**, *13*, 1045−1054.
(41) Cumper, C. W. N.; Thurston, A. P. Electric dipole-moments and molecular conformations of benzophenones, benzils, benzhydrols, and benzoins. *J. Chem. Soc., Perkin Trans. 2* **1972**, 106−111.
(42) Sarphatie, L. A.; Verheijdt, P. L.; Cerfontain, H. Photochemistry of 1,2-diketones. 3. On the luminescence and photochemistry of the lower excited electronic states of some acyclic 1,2-diketones. *Rec. Trav. Chim. Pays-Bas.* **1983**, *102*, 9−13.
(43) Verheijdt, P. L.; Cerfontain, H. Dipole-moments, spectroscopy, and ground and excited-state conformations of cycloalkane-1,2-diones. *J. Chem. Soc., Perkin Trans. 2* **1982**, 1541−1547.
(44) Merritt, E. A.; Bacon, D. J., Raster 3D: Photorealistic molecular graphics. *Meth. Enzymol.* **1997**, *277*, 505−524.
(45) Kraulis, P. J. MOLSCRIPT: A program to produce both detailed and schematic plots of protein structures. *J. Appl. Cryst.* **1991**, *24*, 946−950.

JM0706867